Heat Transport in Herbertsmithite: Can a Quantum Spin Liquid Survive Disorder?

Y. Y. Huang,[1,*] Y. Xu,[2,*,†] Le Wang,[3,*] C. C. Zhao,[1] C. P. Tu,[1] J. M. Ni,[1] L. S. Wang,[1] B. L. Pan,[1] Ying Fu,[3] Zhanyang Hao,[3] Cai Liu,[3] Jia-Wei Mei,[3,4,‡] and S. Y. Li[1,5,6,§]

[1]*State Key Laboratory of Surface Physics, and Department of Physics, Fudan University, Shanghai 200438, China*
[2]*Key Laboratory of Polar Materials and Devices (MOE), School of Physics and Electronic Science, East China Normal University, Shanghai 200241, China*
[3]*Shenzhen Institute for Quantum Science and Engineering, and Department of Physics, Southern University of Science and Technology, Shenzhen 518055, China*
[4]*Shenzhen Key Laboratory of Advanced Quantum Functional Materials and Devices, Southern University of Science and Technology, Shenzhen 518055, China*
[5]*Collaborative Innovation Center of Advanced Microstructures, Nanjing 210093, China*
[6]*Shanghai Research Center for Quantum Sciences, Shanghai 201315, China*

(Received 7 June 2021; accepted 1 December 2021; published 22 December 2021)

One favorable situation for spins to enter the long-sought quantum spin liquid (QSL) state is when they sit on a kagome lattice. No consensus has been reached in theory regarding the true ground state of this promising platform. The experimental efforts, relying mostly on one archetypal material $ZnCu_3(OH)_6Cl_2$, have also led to diverse possibilities. Apart from subtle interactions in the Hamiltonian, there is the additional degree of complexity associated with disorder in the real material $ZnCu_3(OH)_6Cl_2$ that haunts most experimental probes. Here we resort to heat transport measurement, a cleaner probe in which instead of contributing directly, the disorder only impacts the signal from the kagome spins. For $ZnCu_3(OH)_6Cl_2$, we observed no contribution by any spin excitation nor obvious field-induced change to the thermal conductivity. These results impose strong constraints on various scenarios about the ground state of this kagome compound: while certain quantum paramagnetic states other than a QSL may serve as natural candidates, a QSL state, gapless or gapped, must be dramatically modified by the disorder so that the kagome spin excitations are localized.

DOI: 10.1103/PhysRevLett.127.267202

Despite the theoretical appeal of exotic physics in quantum spin liquid (QSL)—long-range quantum entanglement, fractionalized excitations, and emergent gauge structures, the material realization and experimental detection are inevitably riddled with various sources of complications [1–5]. An epitome of this situation is found in the study of the possible QSL physics in herbertsmithite, $ZnCu_3(OH)_6Cl_2$ [6,7]. This material has long been recognized as the most promising candidate for an ideal quantum kagome Heisenberg antiferromagnet (QKHA) [6,7]. As one of the most fundamental questions in frustrated magnetism, determination of the ground state of the QKHA model is challenging already in theory, with numerical evidence supporting various energetically proximate states, including valence bond crystal [8] and gapless or gapped spin liquid [9–24]. Moreover, there is the notorious issue of Cu^{2+} impurities in $ZnCu_3(OH)_6Cl_2$, substantially complicating the interpretation of experimental results [6,7]. Therefore, it remains open questions as to (i) whether and what QSL physics is realized in $ZnCu_3(OH)_6Cl_2$; (ii) what is the role of disorder, and to what extent it modifies the spins in the kagome plane.

Disorder has been a recurring thread in the study of QSL physics [1–3,5]. For instance, the disorder associated with the mixing of Mg^{2+} and Ga^{3+} has been argued to possibly give rise to a mimicry of QSL behaviors in the triangular-lattice QSL candidate $YbMgGaO_4$ [25,26]. In the context of $ZnCu_3(OH)_6Cl_2$, two possible sources of disorder are the Cu substitution on the interlayer Zn sites, and Zn substitution for kagome Cu sites [Fig. 1(a)] [6,7]. Unless specified, we focus on the former, as the existence of the latter remains controversial [27–30]. For most experimental probes, the response can be expressed as $A = A_{\mathrm{imp}} + A^*_{\mathrm{kag}}$, where A is the measured quantity. Such a scheme has been employed in various studies, where A can be the specific heat C [23], the real part of the dynamic spin susceptibility χ' detected by the nuclear magnetic resonance (NMR) shift K [30,31], or the imaginary part χ'' manifested as the spin correlation function S in inelastic neutron scattering (INS) [23] and the spin-lattice relaxation rate $1/T_1$ in NMR [30,31]. The influence of the interlayer Cu^{2+} impurities is twofold: (a) The impurity spins contribute directly to the signal, as represented by A_{imp}. Usually, it is only possible to separate out A_{imp} with novel experimental settings and/or ingenious data processing [23,30]. This forms the main reason why several thermodynamic, INS, and NMR results have led to contradictory interpretations [23,30–41]. (b) The impurity-generated disorder perturbs the environment of the

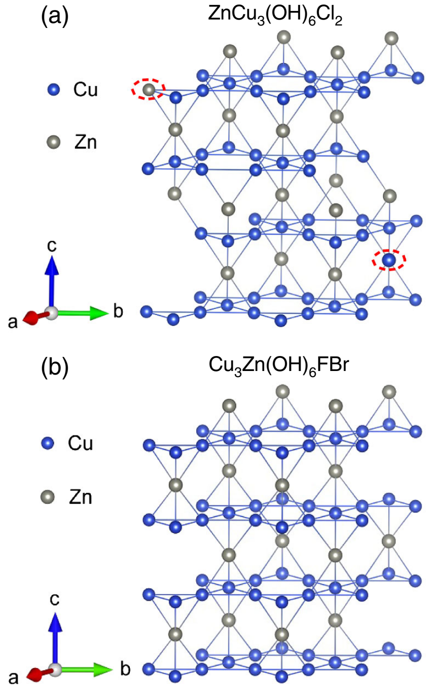

FIG. 1. Schematics of the *ABC*-stacked and *AA*-stacked kagome planes of magnetic Cu^{2+} ions (blue spheres) separated by nonmagnetic Zn^{2+} ions (gray spheres) in (a) $ZnCu_3(OH)_6Cl_2$ and (b) $Cu_3Zn(OH)_6FBr$, respectively. The two sources of disorder for both compounds are shown only in (a) for $ZnCu_3(OH)_6Cl_2$ and highlighted with red circles.

kagome spins, alternating the intrinsic kagome spin contribution A_{kag} in the QKHA model to A^*_{kag} [28,31,37]. The evaluation of this effect also depends on a reliable subtraction of A_{imp}. Note that, the case in which the two terms are intertwined and the additivity fails can be incorporated into (b). Unbiased comparison between the experimental results on $ZnCu_3(OH)_6Cl_2$ and predictions from the QKHA model is not possible without proper consideration of these two aspects, which is highly nontrivial for most experimental probes.

Heat transport measurement of the thermal conductivity κ, on the other hand, is intrinsically free from a direct impurity contribution κ_{imp}. This is evident in $ZnCu_3(OH)_6Cl_2$: First, the impurity sites are dilute, forming nonpercolating spin clusters with no long-range connectivity [23]. Second, the impurity spins were argued to be exchange correlated [23,28], giving rise to dynamical spin fluctuations dominating the low-temperature specific heat and low-energy INS spectra [23]. However, the only role spin fluctuations are able to play in heat transport is to diminish the thermal conductivity by scattering the heat carriers [42,43]. In other words, for the impurity subsystem, there is no connected pathway of any heat carriers, so that $\kappa_{imp} = 0$. Therefore, heat transport measurement on $ZnCu_3(OH)_6Cl_2$ probes only the kagome spins in a surrounding matrix modified by disorder, i.e., κ^*_{kag}. This makes the heat transport measurement, a well-established means in the study of QSL physics [43–57], particularly advantageous in the case of $ZnCu_3(OH)_6Cl_2$.

In this Letter, we performed low-temperature heat transport measurements on high-quality single crystals of $ZnCu_3(OH)_6Cl_2$ and a related kagome QSL candidate, Zn-barlowite, $Cu_3Zn(OH)_6FBr$, recently argued to be an even better realization of the ideal QKHA model [29,58–62]. The absence of a contribution to the thermal conductivity κ from itinerant spin excitations, and the insensitivity of κ to the applied magnetic field, bear profound implications on the possible ground state of these two QSL candidates. Regarding the interplay between disorder and the QSL physics of the kagome spins, previous studies held opposing views, ranging from negligible or weak interplay [23,30], to global symmetry-breaking structural distortions due to local distortions effectively coupled through the correlated kagome spins [28]. Our results unveil a more dramatic manifestation of this interplay: either there are no fractionalized spin excitations in the kagome plane at all; or any kagome spin excitations, should they exist, must be localized in real space.

Single crystals of $ZnCu_3(OH)_6Cl_2$ and $Cu_3Zn(OH)_6FBr$ were grown by a hydrothermal method as in Ref. [63] and Ref. [60], respectively. In contrast to $ZnCu_3(OH)_6Cl_2$, the kagome planes adopt a simple *AA* stacking in $Cu_3Zn(OH)_6FBr$ [58] (Fig. 1). The largest natural surface of the as-grown single crystals of $ZnCu_3(OH)_6Cl_2$ and $Cu_3Zn(OH)_6FBr$ was determined as the (001) plane, i.e., parallel to the kagome planes, by Laue diffraction. Specific heat was measured down to 80 mK using the relaxation method in a Quantum Design physical property measurement system equipped with a small dilution refrigerator. Samples of $ZnCu_3(OH)_6Cl_2$ with dimensions of $0.87 \times 0.39 \times 0.22$ mm^3 (sample 1) and $0.92 \times 0.25 \times 0.11$ mm^3 (sample 2), and a sample of $Cu_3Zn(OH)_6FBr$ with dimensions of $1.25 \times 1.11 \times 0.26$ mm^3, were used for the heat transport measurements. Four silver wires were attached to the (001) plane with silver paint. The heat current is applied perpendicular to the crystallographic *a* axis for $ZnCu_3(OH)_6Cl_2$ (sample 1), and parallel to *a* for $ZnCu_3(OH)_6Cl_2$ (sample 2) and $Cu_3Zn(OH)_6FBr$. Thermal conductivity was measured down to 50 mK in a dilution refrigerator using a standard four-wire steady-state method with two RuO_2 chip thermometers, calibrated *in situ* against a reference RuO_2 thermometer. The magnetic field was applied perpendicular to the (001) plane in both specific heat and thermal conductivity measurements.

The specific heat C of $ZnCu_3(OH)_6Cl_2$ in various applied magnetic fields is displayed in Fig. 2. Compared to previous reports, the specific heat below 0.5 K was measured on single crystals in greater detail for the first time. Although initially fitted to power laws and taken as evidence of gapless spin excitations from the kagome spins [32,33], the low-temperature specific heat was later argued to be unable to reflect the kagome physics [23]. Our results

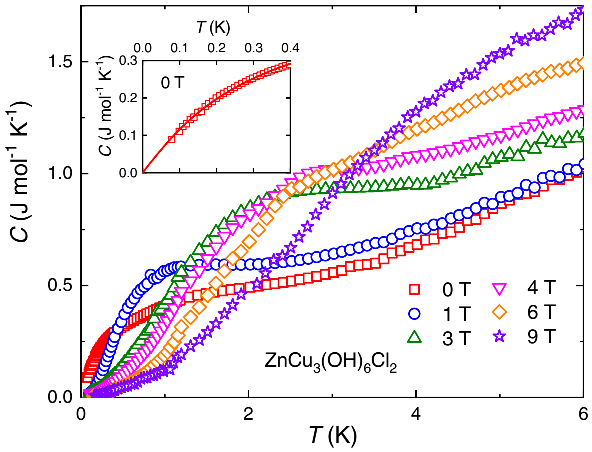

FIG. 2. The specific heat C of $ZnCu_3(OH)_6Cl_2$ in various applied magnetic fields. Inset: Enlarged view of the low-temperature part of the zero-field specific heat. The solid line shows the fitting as in Ref. [23], representing the contribution from the dynamical spin fluctuations associated with the impurity spins. See Sec. I in the Supplemental Material [64] for more details.

are consistent with the scenario that the low-temperature specific heat is dominated by the dynamical fluctuations of the impurity spins [23] (see Sec. I in the Supplemental Material [64]).

The thermal conductivity κ of $ZnCu_3(OH)_6Cl_2$ (sample 1) in various applied magnetic fields is displayed in Fig. 3, while the κ of $ZnCu_3(OH)_6Cl_2$ (sample 2) and $Cu_3Zn(OH)_6FBr$ are compiled in Sec. II in the Supplemental Material [64]. At zero field, we fit the thermal conductivity data to $\kappa/T = a + bT^{\alpha-1}$ below 0.35 K, where the residual linear term $\kappa_0/T \equiv a$ represents the contribution from the spin excitations [43–56]. The fitting gives $\kappa_0/T = -0.023 \pm 0.003$ mW K^{-2} cm^{-1}, and $\alpha = 2.14 \pm 0.02$. The lack of a considerable positive κ_0/T indicates no direct contribution from fermionic spin excitations [43–56], and the value of $2 < \alpha < 3$ is typically attributed to specular reflections of phonons at the sample surfaces [79,80]. However, the 0 T curve shown in Fig. 3(a) evolves from a convex-downward to a convex-upward shape with increasing temperature. Inclusion of higher-temperature data points in the fitting would further decrease the value of κ_0/T and α. Indeed, we show in Sec. III in the Supplemental Material [64] that the absence of a residual linear term holds irrespective of the temperature window for the fitting. The thermal conductivity is seen to be barely responsive to the applied magnetic field, with the largest field-induced change no more than ~8% of the zero-field value, and only evident at higher temperatures, as shown in Fig. 3(c). We demonstrate in Sec. IV in the Supplemental Material [64] that the subtle field-induced increase of κ is not from the direct contribution of kagome spin excitations. The data curves under magnetic field exhibit

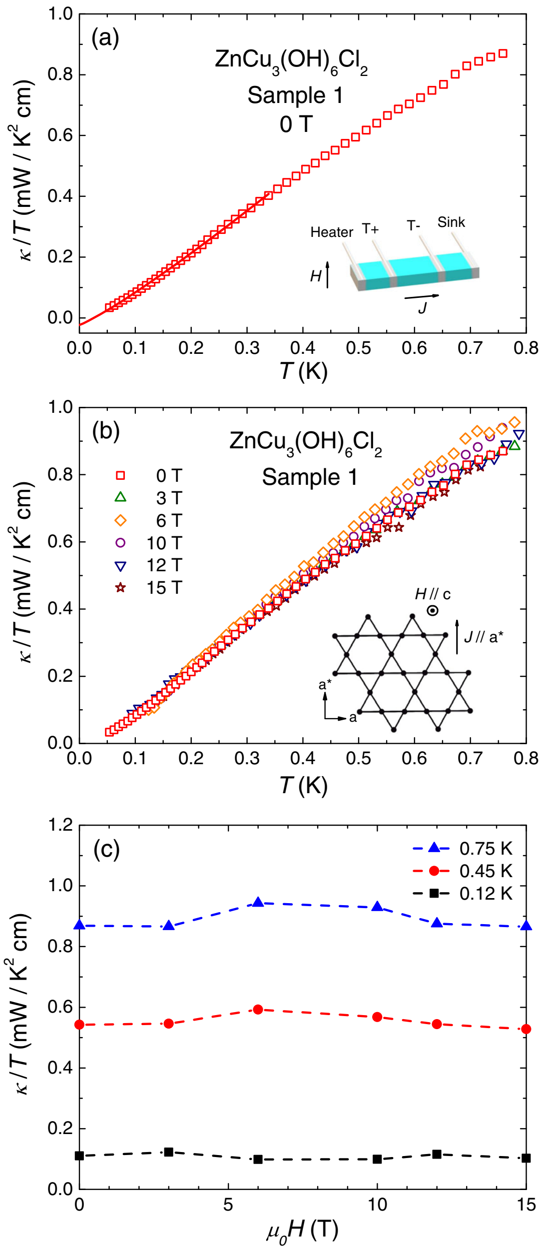

FIG. 3. The thermal conductivity κ of $ZnCu_3(OH)_6Cl_2$ (sample 1) in various applied magnetic fields. The solid line in (a) represents a fit to the zero-field data below 0.35 K by $\kappa/T = a + bT^{\alpha-1}$. The inset in (a) schematically depicts the setup for thermal conductivity measurements, where the four leads in connection with the heater, the thermometers at the higher- and lower-temperature end, and the heat sink are shown. The heat current J flows along the path from the heater to the sink. Note that for each silver wire, the silver paint was applied on all possible surfaces to achieve better thermal contact. The inset in (b) shows the relative direction of J, the direction of the applied magnetic field H, and the crystallographic axes of a kagome lattice. J is parallel to a^* (i.e., perpendicular to a) for $ZnCu_3(OH)_6Cl_2$ (sample 1). The field dependence of κ/T at representative temperatures is shown in (c).

a more pronounced convex-upward shape and, consequently, the fitting yields even more negative κ_0/T and α abnormally smaller than 2. We show in Sec. III in the Supplemental Material [64] that the abnormal values of κ_0/T and α are actually strong evidence for additional scattering of phonons by the magnetic degrees of freedom, as has been demonstrated for other famous QSL candidates like $YbMgGaO_4$ [47], α-$RuCl_3$ [43,53], and $EtMe_3Sb[Pd(dmit)_2]_2$ [51,52]. Overall, in the two kagome QSL candidates $ZnCu_3(OH)_6Cl_2$ and $Cu_3Zn(OH)_6FBr$, for all the field values, there is no direct contribution from kagome spin excitations to the thermal conductivity.

These results are striking, considering the diverse spin excitations predicted from the QKHA model and evidenced by various experimental probes. We now discuss the implications of our results on the possible ground state of $ZnCu_3(OH)_6Cl_2$.

Gapless QSL.—Finite zero-temperature density of states for low-energy spin excitations is expected when spinons form a Fermi surface, giving rise to a finite κ_0/T, which is further modified to a diverging $\kappa/T \sim T^{-2/3}$ ($T \to 0$) when U(1) gauge fluctuations are present [65,66]. In the context of $ZnCu_3(OH)_6Cl_2$, evidence of gapless spin excitations from, e.g., NMR and terahertz conductivity [30,81], has been connected to a U(1) Dirac QSL with fermionic spinons, in which the gap only closes at the Dirac nodes [9–17]. For $\mu_B H \gg k_B T$ (with μ_B the Bohr magneton and k_B the Boltzmann constant), a criterion clearly met by, e.g., our data for $\mu_0 H \gtrsim 6$ T (μ_0 being the vacuum permeability), the Dirac nodes are expected to evolve into Fermi pockets with a radius increasing with field [9]. This would yield a nonzero and increasing κ_0/T with field [82]. Alternatively, a Z_2 QSL with a Dirac spectrum, or Fermi surface, of fractionalized excitations, is predicted to engender a finite κ_0/T or a diverging $\kappa/T \sim T^{-2}$ ($T \to 0$), respectively [87]. The predictions from all the above scenarios are in sharp contrast to our data. The only way to reconcile our results with the existence of gapless kagome spin excitations, is to invoke some mechanisms—presumably associated with the disorder—that would localize these excitations. Note that the excitations are deemed as localized, either when they are strongly scattered so that they cannot propagate along a certain direction at a considerable length scale (e.g., significantly larger than the interspin distance), or they intrinsically exist in closed loops.

Gapped QSL.—For a zero-field spin gap of $\sim$10 K extracted from NMR results [31], the density of thermally excited spin excitations would be negligible in the temperature range of our measurement. The spin gap is expected to decrease with increasing field, and finally closes at $\sim$10 T [31]. In this case, κ is expected to vary significantly with field, and yield a finite κ_0/T for $\mu_0 H \gtrsim 10$ T, inconsistent with our data. Therefore, to come to terms with our results, even gapped kagome spin excitations [18–24] such as gapped spinons and visons in, e.g., a Z_2 short-range resonating valence bond state [19,22,24], must be localized.

Valence bond crystal.—For a valence bond crystal, predicted to be the ground state of the QKHA model in Ref. [8], the lowest triplet excitations are intrinsically confined in real space, hence no contribution to the thermal conductivity.

We now turn to the interplay between disorder and the kagome spins. The analysis on INS and NMR data indicates that the impurity spins appear to have negligible effect on the kagome spins, likely due to their dilute nature [23,30]. However, in contrast to experimental probes where the statistical behavior of the impurity spins or local behavior of a specific site is measured, connected pathways are required for thermal conductivity. In other words, even if the propagation of gapless spin excitations—if they exist—within the kagome plane is hindered only at some breakpoints, i.e., sites close to the impurity spins, heat transport of these excitations may be unable to be established, despite the majority of the kagome spins being unaffected.

A more natural speculation from our results, is that disorder would generate considerable impact on the kagome spins, as implied also by the electron spin resonance results [28]. Generally, impurities in layers adjacent to the magnetic layers are expected to generate disorder in the form of bond randomness, g-factor randomness, Jahn-Teller distortions, etc. In parallel with a scenario of random singlets induced by the interlayer impurity-generated disorder discussed in the context of kagome lattice [88], there is another random-singlet theory encompassing a fraction of spins forming random valence bonds on top of a quantum paramagnetic background [67,89]. In this latter theory, with long-range couplings between the interlayer impurity spins, a random-coupling spin glass behavior might be expected at the lowest temperatures [89]. Consequently, no contribution to the thermal conductivity is expected from spin excitations since they are all frozen. We note that, an elegant demonstration of the interplay between the disorder and the kagome QSL physics was recently reported for Zn-brochantite, $ZnCu_3(OH)_6SO_4$, a QSL candidate possibly featuring a spinon Fermi surface [90–92]. The impurity spins were shown to be Kondo screened by spinons [92]. Since these spinons must be itinerant to induce Kondo screening, an independent check from heat transport measurements on $ZnCu_3(OH)_6SO_4$ would be necessary.

Only the interlayer impurities were considered in the above discussion. One would assume impurities in the kagome layer to be more destructive, since they disturb the frustration motif more directly. Indeed, inclusion of site dilution in the kagome layer in the QKHA model may lead to a valence bond glass phase [93]. Again, such a magnetically frozen phase can be compatible with our results.

In summary, by measuring the low-temperature thermal conductivity of the prototypical kagome QSL candidate $ZnCu_3(OH)_6Cl_2$, we managed to directly probe the kagome spins under the impact of disorder. The absence of a direct magnetic contribution to the thermal conductivity at all fields, and the insensitivity of the thermal conductivity to magnetic field, exclude the existence of itinerant spin excitations. It is not a trivial question whether the framework of a QSL with gapless or gapped spin excitations will break down in the first place, when the emergent spin excitations thereof are constrained to a small length scale. Our results thus call for more attention to scenarios with quantum paramagnetic ground states other than a QSL, such as a valence bond crystal featuring closed-form excitations. A QSL scenario is still viable, if it is associated with loop excitations and closed-form spin dynamics. While on the theory side, deviations from the ideal QKHA Hamiltonian such as exchange and Dzyaloshinskii-Moriya anisotropy may lead to substantial change in the predicted ground state [9,94–96], further complications due to the interplay between disorder and the QSL physics are definitely a crucial aspect to consider when comparing the predictions to experimental results on real materials.

The authors are greatly indebted to Dr. Xiaochen Hong for helpful discussions. This work in Shanghai was supported by the Natural Science Foundation of China (Grant No. 12034004), the Ministry of Science and Technology of China (Grant No. 2016YFA0300503), and the Shanghai Municipal Science and Technology Major Project (Grant No. 2019SHZDZX01). This work in Shenzhen was supported by the program for Guangdong Introducing Innovative and Entrepreneurial Teams (Grant No. 2017ZT07C062), Shenzhen Key Laboratory of Advanced Quantum Functional Materials and Devices (Grant No. ZDSYS20190902092905285), Guangdong Basic and Applied Basic Research Foundation (Grant No. 2020B1515120100) and China Postdoctoral Science Foundation (Grant No. 2020M682780). Y. X. was sponsored by the Shanghai Pujiang Program (Grant No. 21PJ1403100) and the Natural Science Foundation of Shanghai (Grants No. 21JC1402300 and No. 21ZR1420500).

Note added.—Recently, a similar work by Murayama *et al.* appeared [68], in which the observed vanishingly small κ_0/T and field insensitivity of κ are perfectly consistent with our results.

*These authors contributed equally to this work.
†yxu@phy.ecnu.edu.cn
‡meijw@sustech.edu.cn
§shiyan_li@fudan.edu.cn

[1] L. Balents, Spin liquids in frustrated magnets, Nature (London) **464**, 199 (2010).
[2] L. Savary and L. Balents, Quantum spin liquids: A review, Rep. Prog. Phys. **80**, 016502 (2017).
[3] Y. Zhou, K. Kanoda, and T.-K. Ng, Quantum spin liquid states, Rev. Mod. Phys. **89**, 025003 (2017).
[4] J. Knolle and R. Moessner, A field guide to spin liquids, Annu. Rev. Condens. Matter Phys. **10**, 451 (2019).
[5] C. Broholm, R. J. Cava, S. A. Kivelson, D. G. Nocera, M. R. Norman, and T. Senthil, Quantum spin liquids, Science **367**, eaay0668 (2020).
[6] P. Mendels and F. Bert, Quantum kagome antiferromagnet: $ZnCu_3(OH)_6Cl_2$, J. Phys. Conf. Ser. **320**, 012004 (2011).
[7] M. R. Norman, Colloquium: Herbertsmithite and the search for the quantum spin liquid, Rev. Mod. Phys. **88**, 041002 (2016).
[8] R. R. P. Singh and D. A. Huse, Ground state of the spin-$1/2$ kagome-lattice Heisenberg antiferromagnet, Phys. Rev. B **76**, 180407(R) (2007).
[9] Y. Ran, M. Hermele, P. A. Lee, and X.-G. Wen, Projected-Wave-Function Study of the Spin-$1/2$ Heisenberg Model on the Kagomé Lattice, Phys. Rev. Lett. **98**, 117205 (2007).
[10] M. Hermele, Y. Ran, P. A. Lee, and X.-G. Wen, Properties of an algebraic spin liquid on the kagome lattice, Phys. Rev. B **77**, 224413 (2008).
[11] A. C. Potter, T. Senthil, and P. A. Lee, Mechanisms for sub-gap optical conductivity in herbertsmithite, Phys. Rev. B **87**, 245106 (2013).
[12] Y. Iqbal, F. Becca, S. Sorella, and D. Poilblanc, Gapless spin-liquid phase in the kagome spin-$\frac{1}{2}$ Heisenberg antiferromagnet, Phys. Rev. B **87**, 060405(R) (2013).
[13] Y. Iqbal, D. Poilblanc, and F. Becca, Spin-$\frac{1}{2}$ Heisenberg $J_1 - J_2$ antiferromagnet on the kagome lattice, Phys. Rev. B **91**, 020402(R) (2015).
[14] Y.-C. He, M. P. Zaletel, M. Oshikawa, and F. Pollmann, Signatures of Dirac Cones in a DMRG Study of the Kagome Heisenberg Model, Phys. Rev. X **7**, 031020 (2017).
[15] H. J. Liao, Z. Y. Xie, J. Chen, Z. Y. Liu, H. D. Xie, R. Z. Huang, B. Normand, and T. Xiang, Gapless Spin-Liquid Ground State in the $S = 1/2$ Kagome Antiferromagnet, Phys. Rev. Lett. **118**, 137202 (2017).
[16] W. Zhu, X. Chen, Y.-C. He, and W. Witczak-Krempa, Entanglement signatures of emergent Dirac fermions: Kagome spin liquid and quantum criticality, Sci. Adv. **4**, eaat5535 (2018).
[17] W. Zhu, S.-s. Gong, and D. N. Sheng, Identifying spinon excitations from dynamic structure factor of spin-$1/2$ Heisenberg antiferromagnet on the Kagome lattice, Proc. Natl. Acad. Sci. U.S.A. **116**, 5437 (2019).
[18] T. Senthil and M. P. A. Fisher, Z_2 gauge theory of electron fractionalization in strongly correlated systems, Phys. Rev. B **62**, 7850 (2000).
[19] S. Yan, D. A. Huse, and S. R. White, Spin-liquid ground state of the $S = 1/2$ kagome Heisenberg antiferromagnet, Science **332**, 1173 (2011).
[20] S. Depenbrock, I. P. McCulloch, and U. Schollwöck, Nature of the Spin-Liquid Ground State of the $S = 1/2$ Heisenberg Model on the Kagome Lattice, Phys. Rev. Lett. **109**, 067201 (2012).
[21] H.-C. Jiang, Z. Wang, and L. Balents, Identifying topological order by entanglement entropy, Nat. Phys. **8**, 902 (2012).
[22] M. Punk, D. Chowdhury, and S. Sachdev, Topological excitations and the dynamic structure factor of spin liquids on the kagome lattice, Nat. Phys. **10**, 289 (2014).
[23] T.-H. Han, M. R. Norman, J.-J. Wen, J. A. Rodriguez-Rivera, J. S. Helton, C. Broholm, and Y. S. Lee, Correlated

impurities and intrinsic spin-liquid physics in the kagome material herbertsmithite, Phys. Rev. B **94**, 060409(R) (2016).
[24] J.-W. Mei, J.-Y. Chen, H. He, and X.-G. Wen, Gapped spin liquid with Z_2 topological order for the kagome Heisenberg model, Phys. Rev. B **95**, 235107 (2017).
[25] Z. Zhu, P. A. Maksimov, S. R. White, and A. L. Chernyshev, Disorder-Induced Mimicry of a Spin Liquid in $YbMgGaO_4$, Phys. Rev. Lett. **119**, 157201 (2017).
[26] Z. Zhu, P. A. Maksimov, S. R. White, and A. L. Chernyshev, Topography of Spin Liquids on a Triangular Lattice, Phys. Rev. Lett. **120**, 207203 (2018).
[27] D. E. Freedman, T. H. Han, A. Prodi, P. Müller, Q.-Z. Huang, Y.-S. Chen, S. M. Webb, Y. S. Lee, T. M. McQueen, and D. G. Nocera, Site specific x-ray anomalous dispersion of the geometrically frustrated kagomé magnet, Herbertsmithite, $ZnCu_3(OH)_6Cl_2$, J. Am. Chem. Soc. **132**, 16185 (2010).
[28] A. Zorko, M. Herak, M. Gomilšek, J. van Tol, M. Velázquez, P. Khuntia, F. Bert, and P. Mendels, Symmetry Reduction in the Quantum Kagome Antiferromagnet Herbertsmithite, Phys. Rev. Lett. **118**, 017202 (2017).
[29] R. W. Smaha, I. Boukahil, C. J. Titus, J. M. Jiang, J. P. Sheckelton, W. He, J. Wen, J. Vinson, S. G. Wang, Y.-S. Chen, S. J. Teat, T. P. Devereaux, C. Das Pemmaraju, and Y. S. Lee, Site-specific structure at multiple length scales in kagome quantum spin liquid candidates, Phys. Rev. Mater. **4**, 124406 (2020).
[30] P. Khuntia, M. Velazquez, Q. Barthélemy, F. Bert, E. Kermarrec, A. Legros, B. Bernu, L. Messio, A. Zorko, and P. Mendels, Gapless ground state in the archetypal quantum kagome antiferromagnet $ZnCu_3(OH)_6Cl_2$, Nat. Phys. **16**, 469 (2020).
[31] M. Fu, T. Imai, T.-H. Han, and Y. S. Lee, Evidence for a gapped spin-liquid ground state in a kagome Heisenberg antiferromagnet, Science **350**, 655 (2015).
[32] J. S. Helton, K. Matan, M. P. Shores, E. A. Nytko, B. M. Bartlett, Y. Yoshida, Y. Takano, A. Suslov, Y. Qiu, J.-H. Chung, D. G. Nocera, and Y. S. Lee, Spin Dynamics of the Spin-$1/2$ Kagome Lattice Antiferromagnet $ZnCu_3(OH)_6Cl_2$, Phys. Rev. Lett. **98**, 107204 (2007).
[33] M. A. de Vries, K. V. Kamenev, W. A. Kockelmann, J. Sanchez-Benitez, and A. Harrison, Magnetic Ground State of an Experimental $S = 1/2$ Kagome Antiferromagnet, Phys. Rev. Lett. **100**, 157205 (2008).
[34] T. Imai, E. A. Nytko, B. M. Bartlett, M. P. Shores, and D. G. Nocera, ^{63}Cu, ^{35}Cl, and ^{1}H NMR in the $S = \frac{1}{2}$ Kagome Lattice $ZnCu_3(OH)_6Cl_2$, Phys. Rev. Lett. **100**, 077203 (2008).
[35] A. Olariu, P. Mendels, F. Bert, F. Duc, J. C. Trombe, M. A. de Vries, and A. Harrison, ^{17}O NMR Study of the Intrinsic Magnetic Susceptibility and Spin Dynamics of the Quantum Kagome Antiferromagnet $ZnCu_3(OH)_6Cl_2$, Phys. Rev. Lett. **100**, 087202 (2008).
[36] J. S. Helton, K. Matan, M. P. Shores, E. A. Nytko, B. M. Bartlett, Y. Qiu, D. G. Nocera, and Y. S. Lee, Dynamic Scaling in the Susceptibility of the Spin-$1/2$ Kagome Lattice Antiferromagnet Herbertsmithite, Phys. Rev. Lett. **104**, 147201 (2010).
[37] T. Imai, M. Fu, T. H. Han, and Y. S. Lee, Local spin susceptibility of the $S = \frac{1}{2}$ kagome lattice in $ZnCu_3(OD)_6Cl_2$, Phys. Rev. B **84**, 020411(R) (2011).
[38] M. Jeong, F. Bert, P. Mendels, F. Duc, J. C. Trombe, M. A. de Vries, and A. Harrison, Field-Induced Freezing of a Quantum Spin Liquid on the Kagome Lattice, Phys. Rev. Lett. **107**, 237201 (2011).
[39] T. Han, S. Chu, and Y. S. Lee, Refining the Spin Hamiltonian in the Spin-$1/2$ Kagome Lattice Antiferromagnet $ZnCu_3(OH)_6Cl_2$ Using Single Crystals, Phys. Rev. Lett. **108**, 157202 (2012).
[40] T.-H. Han, J. S. Helton, S. Chu, D. G. Nocera, J. A. Rodriguez-Rivera, C. Broholm, and Y. S. Lee, Fractionalized excitations in the spin-liquid state of a kagome-lattice antiferromagnet, Nature (London) **492**, 406 (2012).
[41] G. J. Nilsen, M. A. de Vries, J. R. Stewart, A. Harrison, and H. M. Rønnow, Low-energy spin dynamics of the $s = 1/2$ kagome system herbertsmithite, J. Phys. Condens. Matter **25**, 106001 (2013).
[42] A. F. May, M. A. McGuire, J. E. Mitchell, A. S. Sefat, and B. C. Sales, Influence of spin fluctuations on the thermal conductivity in superconducting $Ba(Fe_{1-x}Co_x)_2As_2$, Phys. Rev. B **88**, 064502 (2013).
[43] Y. J. Yu, Y. Xu, K. J. Ran, J. M. Ni, Y. Y. Huang, J. H. Wang, J. S. Wen, and S. Y. Li, Ultralow-Temperature Thermal Conductivity of the Kitaev Honeycomb Magnet α-$RuCl_3$ across the Field-Induced Phase Transition, Phys. Rev. Lett. **120**, 067202 (2018).
[44] M. Yamashita, N. Nakata, Y. Kasahara, T. Sasaki, N. Yoneyama, N. Kobayashi, S. Fujimoto, T. Shibauchi, and Y. Matsuda, Thermal-transport measurements in a quantum spin-liquid state of the frustrated triangular magnet κ-$(BEDT\text{-}TTF)_2Cu_2(CN)_3$, Nat. Phys. **5**, 44 (2009).
[45] M. Yamashita, N. Nakata, Y. Senshu, M. Nagata, H. M. Yamamoto, R. Kato, T. Shibauchi, and Y. Matsuda, Highly mobile gapless excitations in a two-dimensional candidate quantum spin liquid, Science **328**, 1246 (2010).
[46] Y. Tokiwa, T. Yamashita, M. Udagawa, S. Kittaka, T. Sakakibara, D. Terazawa, Y. Shimoyama, T. Terashima, Y. Yasui, T. Shibauchi, and Y. Matsuda, Possible observation of highly itinerant quantum magnetic monopoles in the frustrated pyrochlore $Yb_2Ti_2O_7$, Nat. Commun. **7**, 10807 (2016).
[47] Y. Xu, J. Zhang, Y. S. Li, Y. J. Yu, X. C. Hong, Q. M. Zhang, and S. Y. Li, Absence of Magnetic Thermal Conductivity in the Quantum Spin-Liquid Candidate $YbMgGaO_4$, Phys. Rev. Lett. **117**, 267202 (2016).
[48] Y. J. Yu, Y. Xu, L. P. He, M. Kratochvilova, Y. Y. Huang, J. M. Ni, L. Wang, S.-W. Cheong, J.-G. Park, and S. Y. Li, Heat transport study of the spin liquid candidate $1T$-TaS_2, Phys. Rev. B **96**, 081111(R) (2017).
[49] I. A. Leahy, C. A. Pocs, P. E. Siegfried, D. Graf, S.-H. Do, K.-Y. Choi, B. Normand, and M. Lee, Anomalous Thermal Conductivity and Magnetic Torque Response in the Honeycomb Magnet α-$RuCl_3$, Phys. Rev. Lett. **118**, 187203 (2017).
[50] J. M. Ni, Q. Y. Liu, Y. J. Yu, E. J. Cheng, Y. Y. Huang, Z. Y. Liu, X. J. Wang, Y. Sui, and S. Y. Li, Ultralow-temperature heat transport in the quantum spin liquid candidate $Ca_{10}Cr_7O_{28}$ with a bilayer kagome lattice, Phys. Rev. B **97**, 104413 (2018).
[51] J. M. Ni, B. L. Pan, B. Q. Song, Y. Y. Huang, J. Y. Zeng, Y. J. Yu, E. J. Cheng, L. S. Wang, D. Z. Dai, R. Kato, and S. Y. Li, Absence of Magnetic Thermal Conductivity in the

Quantum Spin Liquid Candidate $EtMe_3Sb[Pd(dmit)_2]_2$, Phys. Rev. Lett. **123**, 247204 (2019).

[52] P. Bourgeois-Hope, F. Laliberté, E. Lefrançois, G. Grissonnanche, S. R. de Cotret, R. Gordon, S. Kitou, H. Sawa, H. Cui, R. Kato, L. Taillefer, and N. Doiron-Leyraud, Thermal Conductivity of the Quantum Spin Liquid Candidate $EtMe_3Sb[Pd(dmit)_2]_2$: No Evidence of Mobile Gapless Excitations, Phys. Rev. X **9**, 041051 (2019).

[53] R. Hentrich, A. U. B. Wolter, X. Zotos, W. Brenig, D. Nowak, A. Isaeva, T. Doert, A. Banerjee, P. Lampen-Kelley, D. G. Mandrus, S. E. Nagler, J. Sears, Y.-J. Kim, B. Büchner, and C. Hess, Unusual Phonon Heat Transport in α-$RuCl_3$: Strong Spin-Phonon Scattering and Field-Induced Spin Gap, Phys. Rev. Lett. **120**, 117204 (2018).

[54] N. Li, Q. Huang, X. Y. Yue, W. J. Chu, Q. Chen, E. S. Choi, X. Zhao, H. D. Zhou, and X. F. Sun, Possible itinerant excitations and quantum spin state transitions in the effective spin-1/2 triangular-lattice antiferromagnet $Na_2BaCo(PO_4)_2$, Nat. Commun. **11**, 4216 (2020).

[55] B. L. Pan, J. M. Ni, L. P. He, Y. J. Yu, Y. Xu, and S. Y. Li, Specific heat and thermal conductivity of the triangular-lattice rare-earth material $KBaYb(BO_3)_2$ at ultralow temperature, Phys. Rev. B **103**, 104412 (2021).

[56] J. M. Ni, Y. Y. Huang, E. J. Cheng, Y. J. Yu, B. L. Pan, Q. Li, L. M. Xu, Z. M. Tian, and S. Y. Li, Giant isotropic magneto-thermal conductivity of metallic spin liquid candidate $Pr_2Ir_2O_7$ with quantum criticality, Nat. Commun. **12**, 307 (2021).

[57] X. Rao, G. Hussain, Q. Huang, W. J. Chu, N. Li, X. Zhao, Z. Dun, E. S. Choi, T. Asaba, L. Chen, L. Li, X. Y. Yue, N. N. Wang, J.-G. Cheng, Y. H. Gao, Y. Shen, J. Zhao, G. Chen, H. D. Zhou, and X. F. Sun, Survival of itinerant excitations and quantum spin state transitions in $YbMgGaO_4$ with chemical disorder, Nat. Commun. **12**, 4949 (2021).

[58] Z. Feng, Z. Li, X. Meng, W. Yi, Y. Wei, J. Zhang, Y.-C. Wang, W. Jiang, Z. Liu, S. Li, F. Liu, J. Luo, S. Li, G.-q. Zheng, Z. Y. Meng, J.-W. Mei, and Y. Shi, Gapped spin-1/2 spinon excitations in a new kagome quantum spin liquid compound $Cu_3Zn(OH)_6FBr$, Chin. Phys. Lett. **34**, 077502 (2017).

[59] Y. Wei, Z. Feng, W. Lohstroh, D. H. Yu, D. Le, C. d. Cruz, W. Yi, Z. F. Ding, J. Zhang, C. Tan, *et al.*, Evidence for the topological order in a kagome antiferromagnet, arXiv: 1710.02991.

[60] Y. Fu, M.-L. Lin, L. Wang, Q. Liu, L. Huang, W. Jiang, Z. Hao, C. Liu, H. Zhang, X. Shi, J. Zhang, J. Dai, D. Yu, F. Ye, P. A. Lee, P.-H. Tan, and J.-W. Mei, Dynamic fingerprint of fractionalized excitations in single-crystalline $Cu_3Zn(OH)_6FBr$, Nat. Commun. **12**, 3048 (2021).

[61] Y. Wei, X. Ma, Z. Feng, D. Adroja, A. Hillier, P. Biswas, A. Senyshyn, A. Hoser, J.-W. Mei, Z. Y. Meng, H. Luo, Y. Shi, and S. Li, Magnetic phase diagram of $Cu_{4-x}Zn_x(OH)_6FBr$ studied by neutron-diffraction and μSR techniques, Chin. Phys. Lett. **37**, 107503 (2020).

[62] K. Tustain, B. Ward-O'Brien, F. Bert, T. Han, H. Luetkens, T. Lancaster, B. M. Huddart, P. J. Baker, and L. Clark, From magnetic order to quantum disorder in the Zn-barlowite series of $S = 1/2$ kagomé antiferromagnets, npj Quantum Mater. **5**, 74 (2020).

[63] T. H. Han, J. S. Helton, S. Chu, A. Prodi, D. K. Singh, C. Mazzoli, P. Müller, D. G. Nocera, and Y. S. Lee, Synthesis and characterization of single crystals of the spin-$\frac{1}{2}$ kagome-lattice antiferromagnets $Zn_xCu_{4-x}(OH)_6Cl_2$, Phys. Rev. B **83**, 100402(R) (2011).

[64] See Supplemental Material at http://link.aps.org/supplemental/10.1103/PhysRevLett.127.267202 for more details about the fitting and scaling analysis of the specific heat data, thermal conductivity data of $ZnCu_3(OH)_6Cl_2$ (sample 2) and $Cu_3Zn(OH)_6FBr$, fitting of the thermal conductivity data and its physical implications, field-induced change of the thermal conductivity in $ZnCu_3(OH)_6Cl_2$ (sample 1), the sample dependence in the thermal conductivity of $ZnCu_3(OH)_6Cl_2$, the possibility of a striped spin liquid crystal, and hysteresis in thermal conductivity, which includes Refs. [9–17,23,28,32,41,43,45–48,50–56, 58–60,65–78].

[65] S.-S. Lee and P. A. Lee, U(1) Gauge Theory of the Hubbard Model: Spin Liquid States and Possible Application to κ-$(BEDT\text{-}TTF)_2Cu_2(CN)_3$, Phys. Rev. Lett. **95**, 036403 (2005).

[66] C. P. Nave and P. A. Lee, Transport properties of a spinon Fermi surface coupled to a U(1) gauge field, Phys. Rev. B **76**, 235124 (2007).

[67] I. Kimchi, J. P. Sheckelton, T. M. McQueen, and P. A. Lee, Scaling and data collapse from local moments in frustrated disordered quantum spin systems, Nat. Commun. **9**, 4367 (2018).

[68] H. Murayama, T. Tominaga, T. Asaba, A. d. O. Silva, Y. Sato, H. Suzuki, Y. Ukai, S. Suetsugu, Y. Kasahara, R. Okuma, I. Kimchi, and Y. Matsuda, Universal scaling of the specific heat in $S = 1/2$ quantum kagome antiferromagnet herbertsmithite, arXiv:2106.07223.

[69] J. B. Marston and C. Zeng, Spin-Peierls and spin-liquid phases of Kagomé quantum antiferromagnets, J. Appl. Phys. **69**, 5962 (1991).

[70] S. Y. Li, L. Taillefer, C. H. Wang, and X. H. Chen, Ballistic Magnon Transport and Phonon Scattering in the Antiferromagnet Nd_2CuO_4, Phys. Rev. Lett. **95**, 156603 (2005).

[71] L. Messio, B. Bernu, and C. Lhuillier, Kagome Antiferromagnet: A Chiral Topological Spin Liquid? Phys. Rev. Lett. **108**, 207204 (2012).

[72] B. K. Clark, J. M. Kinder, E. Neuscamman, G. K.-L. Chan, and M. J. Lawler, Striped Spin Liquid Crystal Ground State Instability of Kagome Antiferromagnets, Phys. Rev. Lett. **111**, 187205 (2013).

[73] Q. J. Li, Z. Y. Zhao, C. Fan, F. B. Zhang, H. D. Zhou, X. Zhao, and X. F. Sun, Phonon-glass-like behavior of magnetic origin in single-crystal $Tb_2Ti_2O_7$, Phys. Rev. B **87**, 214408 (2013).

[74] T.-H. Han, R. Chisnell, C. J. Bonnoit, D. E. Freedman, V. S. Zapf, N. Harrison, D. G. Nocera, Y. Takano, and Y. S. Lee, Thermodynamic properties of the quantum spin liquid candidate $ZnCu_3(OH)_6Cl_2$ in high magnetic fields, arXiv:1402.2693.

[75] T. Asaba, T.-H. Han, B. J. Lawson, F. Yu, C. Tinsman, Z. Xiang, G. Li, Y. S. Lee, and L. Li, High-field magnetic ground state in $S = \frac{1}{2}$ kagome lattice antiferromagnet $ZnCu_3(OH)_6Cl_2$, Phys. Rev. B **90**, 064417 (2014).

[76] B. Fauqué, X. Xu, A. F. Bangura, E. C. Hunter, A. Yamamoto, K. Behnia, A. Carrington, H. Takagi, N. E. Hussey, and R. S. Perry, Thermal conductivity across the metal-insulator transition in the single-crystalline hyperkagome antiferromagnet $Na_{3+x}Ir_3O_8$, Phys. Rev. B **91**, 075129 (2015).
[77] Z. A. Kelly, M. J. Gallagher, and T. M. McQueen, Electron Doping a Kagome Spin Liquid, Phys. Rev. X **6**, 041007 (2016).
[78] P. Czajka, T. Gao, M. Hirschberger, P. Lampen-Kelley, A. Banerjee, J. Yan, D. G. Mandrus, S. E. Nagler, and N. P. Ong, Oscillations of the thermal conductivity in the spin-liquid state of α-$RuCl_3$, Nat. Phys. **17**, 915 (2021).
[79] M. Sutherland, D. G. Hawthorn, R. W. Hill, F. Ronning, S. Wakimoto, H. Zhang, C. Proust, E. Boaknin, C. Lupien, L. Taillefer, R. Liang, D. A. Bonn, W. N. Hardy, R. Gagnon, N. E. Hussey, T. Kimura, M. Nohara, and H. Takagi, Thermal conductivity across the phase diagram of cuprates: Low-energy quasiparticles and doping dependence of the superconducting gap, Phys. Rev. B **67**, 174520 (2003).
[80] S. Y. Li, J.-B. Bonnemaison, A. Payeur, P. Fournier, C. H. Wang, X. H. Chen, and L. Taillefer, Low-temperature phonon thermal conductivity of single-crystalline Nd_2CuO_4: Effects of sample size and surface roughness, Phys. Rev. B **77**, 134501 (2008).
[81] D. V. Pilon, C. H. Lui, T. H. Han, D. Shrekenhamer, A. J. Frenzel, W. J. Padilla, Y. S. Lee, and N. Gedik, Spin-Induced Optical Conductivity in the Spin-Liquid Candidate Herbertsmithite, Phys. Rev. Lett. **111**, 127401 (2013).
[82] There are alternative proposals that the field-induced phase with spinon Fermi pockets is unstable to a spin solid phase [10,38,83–86]. A decreasing thermal conductivity with increasing field is expected for this case, since the gapless Dirac spinons are present only in the Dirac spin liquid phase at zero and low field, and the spin gap in the spin solid phase increases with field [38].
[83] Y. Ran, W.-H. Ko, P. A. Lee, and X.-G. Wen, Spontaneous Spin Ordering of a Dirac Spin Liquid in a Magnetic Field, Phys. Rev. Lett. **102**, 047205 (2009).
[84] O. Cépas, C. M. Fong, P. W. Leung, and C. Lhuillier, Quantum phase transition induced by Dzyaloshinskii-Moriya interactions in the kagome antiferromagnet, Phys. Rev. B **78**, 140405(R) (2008).
[85] L. Messio, O. Cépas, and C. Lhuillier, Schwinger-boson approach to the kagome antiferromagnet with Dzyaloshinskii-Moriya interactions: Phase diagram and dynamical structure factors, Phys. Rev. B **81**, 064428 (2010).
[86] Y. Huh, L. Fritz, and S. Sachdev, Quantum criticality of the kagome antiferromagnet with Dzyaloshinskii-Moriya interactions, Phys. Rev. B **81**, 144432 (2010).
[87] Y. Werman, S. Chatterjee, S. C. Morampudi, and E. Berg, Signatures of Fractionalization in Spin Liquids from Interlayer Thermal Transport, Phys. Rev. X **8**, 031064 (2018).
[88] H. Kawamura, K. Watanabe, and T. Shimokawa, Quantum spin-liquid behavior in the spin-1/2 random-bond Heisenberg antiferromagnet on the kagome lattice, J. Phys. Soc. Jpn. **83**, 103704 (2014).
[89] I. Kimchi, A. Nahum, and T. Senthil, Valence Bonds in Random Quantum Magnets: Theory and Application to $YbMgGaO_4$, Phys. Rev. X **8**, 031028 (2018).
[90] M. Gomilšek, M. Klanjšek, M. Pregelj, F. C. Coomer, H. Luetkens, O. Zaharko, T. Fennell, Y. Li, Q. M. Zhang, and A. Zorko, Instabilities of spin-liquid states in a quantum kagome antiferromagnet, Phys. Rev. B **93**, 060405(R) (2016).
[91] M. Gomilšek, M. Klanjšek, M. Pregelj, H. Luetkens, Y. Li, Q. M. Zhang, and A. Zorko, μSR insight into the impurity problem in quantum kagome antiferromagnets, Phys. Rev. B **94**, 024438 (2016).
[92] M. Gomilšek, R. Žitko, M. Klanjšek, M. Pregelj, C. Baines, Y. Li, Q. M. Zhang, and A. Zorko, Kondo screening in a charge-insulating spinon metal, Nat. Phys. **15**, 754 (2019).
[93] R. R. P. Singh, Valence Bond Glass Phase in Dilute Kagome Antiferromagnets, Phys. Rev. Lett. **104**, 177203 (2010).
[94] A. Zorko, S. Nellutla, J. van Tol, L. C. Brunel, F. Bert, F. Duc, J.-C. Trombe, M. A. de Vries, A. Harrison, and P. Mendels, Dzyaloshinsky-Moriya Anisotropy in the Spin-$\frac{1}{2}$ Kagome Compound $ZnCu_3(OH)_6Cl_2$, Phys. Rev. Lett. **101**, 026405 (2008).
[95] A. Zorko, F. Bert, A. Ozarowski, J. van Tol, D. Boldrin, A. S. Wills, and P. Mendels, Dzyaloshinsky-Moriya interaction in vesignieite: A route to freezing in a quantum kagome antiferromagnet, Phys. Rev. B **88**, 144419 (2013).
[96] C.-Y. Lee, B. Normand, and Y.-J. Kao, Gapless spin liquid in the kagome Heisenberg antiferromagnet with Dzyaloshinskii-Moriya interactions, Phys. Rev. B **98**, 224414 (2018).